JAAS

Accepted Manuscript

This is an *Accepted Manuscript*, which has been through the Royal Society of Chemistry peer review process and has been accepted for publication.

Accepted Manuscripts are published online shortly after acceptance, before technical editing, formatting and proof reading. Using this free service, authors can make their results available to the community, in citable form, before we publish the edited article. We will replace this *Accepted Manuscript* with the edited and formatted *Advance Article* as soon as it is available.

You can find more information about *Accepted Manuscripts* in the Information for Authors.

Please note that technical editing may introduce minor changes to the text and/or graphics, which may alter content. The journal's standard Terms & Conditions and the Ethical guidelines still apply. In no event shall the Royal Society of Chemistry be held responsible for any errors or omissions in this *Accepted Manuscript* or any consequences arising from the use of any information it contains.

ROYAL SOCIETY OF CHEMISTRY

www.rsc.org/jaas

Analysis of Mass Dependent and Mass Independent Selenium Isotope Variability in Black Shales

Philip A.E. Pogge von Strandmann[1,2], Christopher D. Coath[1], David C. Catling[1,3], Simon W. Poulton[4], Tim Elliott[1]

[1]Bristol Isotope Group, School of Earth Sciences, Bristol University, Wills Memorial Building, Queen's Road, Bristol, BS8 1RJ, UK

[2]Institute of Earth and Planetary Sciences, University College London and Birkbeck, University of London, Gower Street, London, WC1E 6BT, UK

[3]Department of Earth and Space Sciences, University of Washington, Seattle, WA 98195, USA

[4]School of Earth and Environment, University of Leeds, Leeds, LS2 9JT, UK

Abstract

The measurement of selenium isotope ratios is of increasing interest for understanding redox conditions in present and past surface environments. Se has six stable isotopes, and is therefore well suited for isotope analysis by double spiking. However due to relatively large interferences on every isotope, and complex chemical purification methods that frequently do not generate 100% yields, rigorously determining the accuracy of measurements is critical. Here we present analyses of USGS shale standards (SCo-1 and SGR-1b), as representatives of material which might be of interest to Se isotope studies. We have made analyses using two separate double spikes (^{74}Se-^{78}Se and ^{78}Se-^{82}Se), and compare them to previously published results. In addition, we present models of the effects of uncorrected interferences on double

spike inversions. This leads us to propose $\delta^{82/76}$Se (parts per thousand deviation of ^{82}Se/^{76}Se from NIST SRM-3149) values of -0.22 ± 0.15 for SCo-1, and +0.25 ± 0.17 for SGR-1b. Further, we present a new method of measuring Se isotopes by desolvation nebulisation. Se sensitivity is enhanced by a factor of 100-200 times by doping solutions with pure Mg, leading to almost a factor of two less material required compared to the more standard hydride generation. Interferences are different compared to our standard hydride generation protocol, but analyses of double spiked NIST-3149 shows that this method can generate accurate isotope ratios. Finally, mass independent fractionation (MIF) of sulphur isotopes has generated considerable interest for constraining the early oxygenation of the atmosphere. Given the chemical similarities between S and Se, Archean shales with S MIF might be expected to exhibit Se MIF. However, within our analytical uncertainty of ±0.4-0.5‰ (parts per 10,000), there is no resolvable Se MIF in these samples, indicating different atmospheric cycling of Se and S.

Keywords

Ocean redox; Se isotopes; black shales; mass dependent fractionation; mass independent fractionation; hydride generation; desolvation

1.0 Introduction

Selenium and its stable isotopes are increasingly generating interest in the geochemical community for their potential to trace present and past surface water redox processes[1-7]. As for S, microbial reduction of Se is thought to be the dominant cause of natural Se isotope fractionation[3, 8]. The chemistries of S and Se have notable similarities but, significantly, the redox transitions between the highest naturally

occurring oxidation state of selenium, Se(VI), and its common reduced forms, Se (IV), Se(0) and Se(-II), occur at higher pE than for the dominant sulphur redox states, S(VI) and S(-II)[3, 6, 9-12]. Selenium isotope measurements may therefore be suited to trace changes in ocean redox at relatively oxidised conditions, after the great oxidation event.

Of the existing means of analysis, gas-source spectrometry requires prohibitively large quantities of Se[6]. Negative thermal ionisation mass spectrometry has proven to be useful[2], but it has only been since the development of multi-collector plasma ionisation mass spectrometers that interest in Se isotope measurements for geochemical purposes has begun to grow[13]. Even so, Se ionises poorly in a plasma and Se is generally introduced as a Se-hydride gas, thereby avoiding the sensitivity loss due to a hydrous carrier matrix[13, 14]. However, hydride generation has its own inherent problems, as elements that directly interfere with Se isotopes (e.g. Ge, As), as well as those that may cause matrix effects (e.g. Sb), also readily form hydrides, and therefore pre-analysis chemical purification must take place, as well as interference corrections. Coupled with interferences stemming from the plasma carrier gas (ArAr and Kr), these factors make Se isotope measurements challenging.

Purification chemistry for Se from common geological matrices has been described by a number of authors, using the now fairly well established thiol cotton fibre method[7, 9, 13, 15-17]. However, given the difficulty in obtaining 100% yields from this chemistry, the potential exists for isotopic fractionation of the sample to occur during sample preparation. This concern can be circumvented by using a double-spiked approach, which corrects for any mass-dependent fractionation during sample processing if the samples and spike are equilibrated prior to chemical purification[1, 3, 7, 14, 16, 18-21]. Double spiked analyses are also robust against possible differential

instrumental fractionation of samples with residual matrix compared to clean solution standards, which is a major consideration in sample-standard bracketing methods. Selenium has six stable isotopes, apparently providing ample choice for selecting the four isotopes required for double spiked analysis. The potential drawback of this method, however, is that at these four isotopes must be fully corrected for any interferences, compared to only two required in sample-standard bracketing. The benefits of double spiking outlined above should outweigh those of sample-standard bracketing in measuring mass dependent isotope variability, but interferences must be resolved or accurately corrected. Here we examine a number of these issues, with reference to our own work and to also to different studies in the literature.

Since Se is strongly associated with organic matter[8, 22, 23], shale is the most commonly used rock type for Se isotope analyses of ancient past environments. Therefore well-characterised shale standards are required in order for Se isotope studies to be cross-calibrated. However, published values for the common USGS shale standard SGR-1 differ by up to 0.74‰ on the $^{82}Se/^{76}Se$ ratio[7, 13, 17, 19, 24, 25]. Here we examine the Se isotope composition of two USGS shales (SGR-1 and SCo-1) with multiple, independently constrained, double spike inversions, with the aim of providing useful isotopic reference compositions. We also examine some Archean rocks for the potential of Se mass independent fractionation (MIF), given the presence of sulphur MIF in these rocks.

2.0 Double spike

Selenium has six stable isotopes (given that ^{82}Se has a half life of $\sim 10^{20}$ years and can be considered stable): ^{74}Se, ^{76}Se, ^{77}Se, ^{78}Se, ^{80}Se and ^{82}Se. Their natural abundances are detailed in Table 1. Two separate double spikes were trialled in this

study. Both were made up from enriched single isotope standards from Cambridge Isotope Laboratories, Inc., with certified enrichment factors between 92% for ^{82}Se, 97% for ^{78}Se and >99% for ^{74}Se. The enriched material was dissolved individually in concentrated HNO_3 to ensure no reductive loss of Se, diluted, and then mixed gravimetrically, according to the compositions suggested by the Double Spike Toolbox[26]. The double spikes were calibrated by standard addition, by mixing NIST-3149 and the double spike in various proportions, which were then used to constrain the pure spike composition. This composition was also verified by measuring a pure double spike by sample-standard bracketing with NIST-3149.

Initially we used a ^{74}Se-^{78}Se spike (calibrated ratios: ^{74}Se/^{78}Se =0.856, ^{74}Se/^{77}Se =90.445, ^{78}Se/^{77}Se =105.645), with ^{77}Se and ^{82}Se as the other isotopes for the inversion. This approach has the disadvantage that it has a significant Ge interference on ^{74}Se, which can be up to 70% of the signal. We also used a ^{78}Se-^{82}Se spike (calibrated ratios: ^{78}Se/^{82}Se =0.185, ^{78}Se/^{76}Se =110.847, ^{82}Se/^{76}Se =598.23), with an inversion scheme that additionally uses ^{76}Se and ^{77}Se measurements. The latter procedure allows analyses at lower Se intensities, because the interfered ^{74}Se is not required. However, it does use ^{76}Se, which has three significant interferences: ^{40}Ar^{36}Ar, ^{76}Ge and ^{75}AsH, albeit the sum of these contributions is typically smaller (~3–10%) relative to the mass 76 intensity than ^{74}Ge to mass 74. The ^{78}Se-^{82}Se spike was used most extensively, although results from both spikes are presented below to provide multiple constraints on the compositions of the shale standards.

All isotope ratios are presented as $\delta^{82/76}$Se, which is the ‰ deviation of the ^{82}Se/^{76}Se ratio of the sample from that of NIST SRM-3149 (Lot No. 992106). This reference material is a NIST 10.042 ± 0.051 mg/g single element standard solution, which is not isotopically certified, although its absolute composition has been

reported[27], and has become the isotopic reference standard of choice for Se[1, 5, 7, 17, 19, 28]. Our standard is from the same lot as for some other studies[5, 17, 28]. The ^{74}Se-^{78}Se double spike inversion does not use ^{76}Se, so these ratios are converted to $\delta^{82/76}$Se notation from $\delta^{82/77}$Se using the exponential mass fractionation law.

Concentrations of samples were determined by isotope dilution as part of the double spike inversion, with an inaccuracy of ±4% (likely dominated by weighing inaccuracy), as determined by repeat analyses of the USGS shales described below.

3.0 Experimental

3.1 Hydride-generation MDF chemistry

The chemical purification of Se for both isotope ratio analysis and isotope dilution has been well described in a number of studies. In general we follow the methods of Rouxel et al. (2002) and Elwaer and Hintelmann (2008). Briefly, this involves dissolution of the powdered shale samples in repeated steps of HF-HNO_3 and HNO_3-H_2O_2, without exceeding 80°C in order to avoid loss of Se by volatilisation. The double spike was normally introduced to the sample at the end of dissolution (during the final HNO_3 step to allow spike-sample equilibration), but before chemistry, so as to be able to respike the same dissolved material if initial sample/spike mixtures were sub-optimal. Our experiments show that identical isotope ratios and concentrations result from adding the spike at various stages during dissolution. Because shales can contain a significant amount of organic matter, we also experimented with dissolution of rock powders at high temperature and pressure, using an Anton-Paar HPA-S ashing system (2 hours at 220°C and 100 bar, in concentrated HF and HNO_3).

Following dissolution, the samples were reduced in 4 M HCl for 1 hour at 80°C, and then passed three times through 0.2 g of Thioglycollic Cotton Fibre (TCF)[13]. Se was then desorbed from the TCF by placing the TCF in a centrifuge tube with 1 ml concentrated HNO_3 and then heating the tube in a boiling water bath for 20 minutes. The oxidised TCF was then diluted with 3 ml MQ H_2O and centrifuged. Multiple extractions ensure higher yields, but also dilute the sample more, because completely drying the sample down can cause the formation of insoluble thiol salts. It is, however, possible to extract Se several times (typically three times), and dry the resulting solution down to a pre-determined volume, in order to increase the Se concentration in the solution (by decreasing the solution volume). Following this, concentrated HCl was added to make the sample up to 1.6M HCl, and heated at 80°C for one hour, to reduce the Se(VI) to Se(IV), ready for hydride generation[14, 16, 17]. Yields of 100% can be obtained for experiments with pure Se, but comparisons of Se beam intensity on the mass spectrometer with concentrations derived from the double spike inversion clearly show that additional matrix can lead to lower yields. The yields from purifying shale samples are ~80–100%[1], and can vary randomly with individual samples. This would likely not be observable in this, or indeed in other, studies unless some form of isotopic spiking were involved. Ashing samples leads to lower yields (50–60%), possibly because the high temperatures cause Se loss, as described elsewhere[13, 29]. However, this effect does not cause resolvable differences in the isotope ratio, due to addition of double spike prior to ashing. The total procedural blank from this method is ~0.4 pg Se, which is too low to determine a typical blank isotope ratio.

The TCF chemistry efficiently removes major elements (e.g. post-chemistry Al/Se of SCo-1 ~ 10^{-5}, determined on a Thermo Finnigan Element 2 sector-field ICP-

MS, by calibrating against a set of synthetic multi-element standards), as well as matrix elements that could compete for hydride generation (S/Se of SCo-1 is reduced from ~700 to 0.002 by chemical purification, a similar final ratio to NIST 3149). Complete elemental scans of purified SCo-1 have showed that Sb has relatively high post-chemistry abundance (Sb/Se reduced from 2.8 to 0.01). Such matrix effects should not affect double spiked measurements, but may influence sample-standard bracketing (SSB), because Sb forms hydrides relatively easily[13], and therefore its possible influence should be monitored in SSB studies. Abundances of elements with nuclides that isobarically interfere with the Se isotope spectrum are also reduced by the chemistry: As/Se in SCo-1 is reduced from 13.5 to 0.01, and Ge/Se from 1.7 to 10^{-4}. Nevertheless these abundances are sufficient to cause significant perturbation of the Se isotope ratios if not corrected and this effect can be greater in other shale samples as both As/Se and Ge/Se can be several orders of magnitude higher than in SCo-1 and SGR-1.

3.2 Analyses

All analyses were performed on a Thermo Finnigan multicollector inductively coupled plasma mass spectrometer, with a hydride-generation introduction system (HG-MC-ICP-MS) in the laboratories of the Bristol Isotope Group, University of Bristol. In order to reduce levels of oxide and hydride interferences, standard "H" skimmer cones were used, rather than the more sensitive "X" cones. Since various NiO isotopologues produced from commonly used Ni cones can interfere on Se isotopes (e.g. $^{58}Ni^{16}O$ ~0.03 pA, typically ~0.2–1% of the ^{74}Se beam), all cones used were aluminium, which reduced the intensity of $^{58}Ni^{16}O$ by an order of magnitude.

This also has the advantage of a ~15% sensitivity increase, likely because of the higher working temperatures of Al cones.

Samples were introduced using a Cetac HGX 200 hydride generator. This system features a frosted glass rod that allows enhanced mixing between the sample and the hydride forming reagent ($NaBH_4$) and therefore a high efficiency of Se-hydride generation. However, this system also has the disadvantage that the frosted glass rod causes long wash-out times – on the order of tens of minutes to obtain natural ratios after spiked samples. In order to avoid using large volumes of rinse acid, ~75% of this rinse was performed while aspirating air, leaving the continuously pumped $NaBH_4$ to clean the glass rod.

At the beginning of an analytical session, the samples were taken up into 1.6 M HCl, ready for introduction into the hydride generator. For analysis, samples were mixed with 1% $NaBH_4$ dissolved in 0.014 M NaOH in the hydride generator. All solutions were pumped through the hydride generator, using a multi-channel peristaltic pump. Using an uptake rate of ~300 μl/min, a 200 ng/ml Se solution gave an intensity of ~30 pA on ^{76}Se. Including uptake time, the analyses requires 2 ml of sample and ideally a total of 400 ng of Se. Up to 3–4 times less Se can be analysed, although uncertainty begins to increase at the lower end of this spectrum, as the role of interferences starts to become critical (see Section 4.1). The amount of Se required is generally similar to, or slightly higher, than reported by other recent studies[7, 17, 19], and considerably more than reported for a collision-cell instrument[13]. Interestingly, this is the first Se isotope study to employ a Neptune, rather than Nu or Isoprobe MC-ICP-MS, potentially hinting that the relative sensitivity for interferences (such as argides, as detailed in Section 4.1) is somewhat higher on a Neptune. All measurements were bracketed with on-peak background measurements, and double-

spiked NIST-3149 was analysed every 3–4 measurements. Each individual sample and blank measurement consisted of 50 ratios (210 s integration time).

4.0 Interference corrections

A series of interference corrections were performed on measured samples. The justification and evaluation of these corrections are detailed below but, briefly, analyses were background corrected, to remove contributions from the plasma gas and carrier matrix, followed by correction for Ge, SeH and AsH interferences. Most of these corrections are standard for Se isotope analysis[6, 7, 13, 14, 17, 18, 30], although we explore potential pitfalls in these corrections to a greater degree than previous studies. The formulae used for the novel approach of simultaneous correction of these interferences, together with the double spike inversion, are given in the appendix.

All nine faraday cups of the Neptune were used for the measurements, which allowed analysis of all Se isotopes and requisite Se-free isobaric interferences without peak jumping. The dominant beams collected in each cup, including the main interferences, are detailed in Table 1.

4.1 ArAr corrections (background correction)

Argon dimers from the plasma gas interfere on several Se isotopes. Most notably, typical $^{40}Ar^{40}Ar$ intensities of ~40 pA mean that its influence on ^{80}Se cannot be accurately corrected, but this is not the case for the minor Ar dimers. The most straightforward method for correcting for Ar dimer interference is by subtracting the background measured in clean acid ("on-peak background"). It is alternatively possible to correct for ArAr by measuring the ^{80}Se-corrected $^{40}Ar^{40}Ar$ beam, and using this to calculate the other ArAr beams[5, 17]. However, this method would require

an appropriate functional relationship between $^{40}Ar^{40}Ar$ and the other dimers; an assumption of an exponential mass dependent relationship as used for elemental species might be the most obvious. Although the exponential form is widely used for inter-relating atomic species its effectiveness for dimers is not well documented and need not necessarily be similarly appropriate. Further complications arise from the need to correct for ^{80}Kr or ^{79}BrH interferences on mass 80.

In contrast, an 'on-peak' background correction has the advantage that all machine-generated backgrounds are corrected (i.e. also those from Kr and ArArH), but this approach requires long wash-out times (up to 45-60 min) in order to return to a normal background after analysis of a spiked solution. An assumption also needs to be made that the ArAr beams remain identical when aspirating Se-bearing and Se-free acidic solutions, although this is a common approach in MC-ICP-MS. However, we have tested this assumption, by connecting the hydride generator to an Element 2 ICP-MS run at high resolution ($M/\Delta M \sim 10{,}000$, 5-95% peak edge width), with which it is possible to resolve Se and ArAr peaks (albeit with a loss of almost an order of magnitude of sensitivity). As shown in Figure 1, the ArAr peaks remain at the same intensity whether there is a Se peak present or not, justifying the use of a background correction. The $^{40}Ar^{37}Cl$, which is entirely dominated by the HCl matrix, interference on mass 77 is similarly corrected. The potential effect of uncorrected ArAr interferences is further explored in Section 4.4.

Nevertheless, a minimum Se intensity threshold is necessary, below which the background intensities of even the minor dimers, particularly $^{36}Ar^{40}Ar$ (typically ~0.3 pA), cannot be corrected for with sufficient accuracy. A 10% background contribution to the measured mass 76 intensity, using our inversion including ^{76}Se, causes a ~2.5‰ $\delta^{82/76}Se$ inaccuracy in measurements on NIST SRM-3149 (Fig. 2), whereas for a

background contribution of ~5% the measurements are within error of the reference value. In contrast, the $^{38}Ar^{40}Ar$ background does not exceed ~0.1% of the 78 beam in either double spike system and therefore does not compromise the analyses.

4.2 Ge corrections

Germanium-73 was monitored to correct for Ge interferences on ^{74}Se and ^{76}Se. Since fractionation of Se and Ge are likely subtly different, this correction will likely only work well at low Ge/Se relative abundances. It is therefore critical that tests were undertaken using Se standards doped with variable amounts of Ge to establish the limit of Ge/Se at which the correction is robust. The results of these tests, shown in Figure 3, demonstrate that a Se mass bias can be used to correct Ge interferences accurately up to a Ge/Se intensity ratio of ~0.1 in the purified samples. The analysed Se fractions of the shale standards reported here have Ge/Se < 0.05 (mostly <0.03). Such correction problems are likely duplicated in any method that uses the Se mass bias to correct Ge interferences, and studies analysing samples with higher post-chemistry Ge/Se should monitor two Ge isotopes for accurate mass bias generation.

4.3 Hydride corrections (AsH, SeH, GeH, ArArH)

The use of a hydride generator results in large amounts of free hydrogen gas entering the plasma, which may subsequently bind to other elements introducing hydride molecular ions into the mass spectrometer. The method we employ to correct for hydride ions is to determine the degree of SeH formation by monitoring the background-corrected ^{82}Se and mass 83, assumed to consist of only ^{82}SeH. The background correction ("on-peak background") on mass 82 corrects for ^{82}Kr and ^{81}BrH, assuming Br dominantly stems from the carrier matrix (HCl), based on scans

via an Element 2 ICP-MS, and on mass 83 corrects for ^{83}Kr interference. Depending on the tuning of the hydride generator (e.g. concentrations of $NaBH_4$) and of the mass spectrometer, the resulting SeH/Se is ~ 10^{-3} to 10^{-4}. Typically, tuning was optimised to minimise hydride formation. The correction of ^{76}SeH on ^{77}Se, and of ^{77}SeH on ^{78}Se is straightforward (see Appendix). The hydride correction is mass bias corrected for the difference in mass between ^{82}Se/^{82}SeH and the other hydride-forming isotopes.

Arsenic hydride is a significant interference on ^{76}Se. For example, an uncorrected AsH interference at an As/Se = 0.2 will decrease the final δ^{8276}Se by 1 to 5‰, depending on the sample introduction and mass spectrometer tuning. Since As is monoisotopic we assume, out of necessity, that the As/AsH ratio is identical to ^{82}Se/^{82}SeH. This relationship has been assessed using tests with the NIST-3149 standard doped with As, with ratios up to As/Se ~ 1.5 (As/^{76}Se ~ 16; Fig. 4). Post chemistry, samples rarely exceed As/Se ~ 0.3 but occasionally shales with very high original As/Se (>100) may exceed this. Such samples were discarded, as the influence of the interference is uncalibrated at such ratios, although it is possible that the correction will still be accurate.

Doping experiments have also shown that the GeH/Ge ratio is identical within uncertainty to that of SeH/Se (separate analyses of GeH formation (^{74}Ge/^{74}GeH) from a pure Ge solution and SeH formation from a pure Se solution performed within a few minutes of each other, with the same tuning parameters). However, given the low abundance of Ge in purified samples (typically ~0.1 pA on mass 73), no GeH correction was performed.

A further interfering hydride on the Se isotopic spectrum is ArArH. The degree of argide dimer hydride formation is different from that of SeH formation. We determined this from measurements of ^{40}Ar^{40}ArH/^{40}Ar^{40}Ar at 'medium resolution'

(M/ΔM ~ 6000, 5-95% peak edge width), which resolves the hydride from ^{81}Br. We found ArArH/ArAr ~ 0.01, 1–2 orders of magnitude greater than SeH/Se, which makes direct correction difficult because, given the number of faraday cups on a Neptune, a peak jump would have to be performed to measure the degree of argide dimer hydride formation at mass 81. Our observations on ArArH formation, however, have a bearing on studies that perform argide corrections based on the beam at mass 80 (e.g.[17, 21]), rather than a background correction, unless, for example, this is experimentally calibrated[17]. Fortunately, as demonstrated above, the levels of argide dimer, and therefore also the levels of ArArH, are identical within measurement uncertainty in blank acid and sample and, therefore, ArArH is also corrected for in the background subtraction. The formulae for the simultaneous correction of all the above interferences as part of the double spike inversion are given in the appendix.

4.4 Double spike interference models

Although individual interferences can be corrected in the tests described above, it is nevertheless necessary to determine whether natural samples have had all interferences corrected. Generally this is hard to accomplish, especially with an isotopic system with few published studies or standards. However, the effectiveness of our correction procedure can be checked by spiking a natural sample with variable amounts of double spike, to generate different spike/sample ratios (f_{spike} - defined as the mixture M in Rudge et al., 2009). Clearly, consistent results should be obtained regardless of f_{spike}, if the interferences are correctly accounted for. These results can also be compared with a similar test conducted on a variably spiked pure Se standard. Since double spike inversions respond non-linearly to interferences, and because changing the sample/spike ratio effectively varies the ratio of potential interferences

to Se (at very high f_{spike} only two Se isotopes are present, whereas at very low f_{spike} Se is present in virtually natural abundances), a large f_{spike} range provides the opportunity to test the accuracy of the isotopic data.

The results of variably spiking NIST-3149 and the USGS shales SGR-1 and SCo-1 are shown in Figure 5. This exercise not only shows the optimal sample/spike ratio ("cocktail"[26]), but also shows that isotope ratios resulting from variable spiking of the NIST standard and variable spiking of shales coincide. This demonstrates that all interferences, both instrumental- and sample-generated, are fully corrected for. In order to demonstrate how sensitive spiked samples are to uncorrected interferences, we also show forward models for the ^{78}Se-^{82}Se double spike inversion with uncorrected interferences on various isotopes. Clearly the isotope with the greatest potential for uncorrected interferences is ^{76}Se (in an inversion using ^{76}Se, ^{77}Se, ^{78}Se and ^{82}Se), where explicit ^{76}Ge and ^{75}AsH corrections are required on top of a significant back-ground correction (for $^{40}Ar^{36}Ar$). The variability of $\delta^{82/76}Se$ against f_{spike} (Fig. 6) in models with incompletely corrected interference is strikingly different from the invariant results of rock standards run at different f_{spike}, demonstrating that these interferences are correctly accounted for in the samples. This model indicates that even an uncorrected 1‰ (0.1%) interference on ^{76}Se can push the final $\delta^{82/76}Se$ by several permil from the true ratio, which demonstrates the necessity for careful interference correction. Modelling shows that the effect of the more minor argon dimer isotopologues is insignificant compared to that of $^{40}Ar^{36}Ar$.

Figure 6 also shows the model results for an uncorrected interference at mass 82, which affects the $\delta^{82/76}Se$ to a lesser extent, but still demonstrates that any existing interferences are fully corrected in our data reduction.

5.0 Analytical Results and Discussion

5.1 Shale $\delta^{82/76}$Se and analytical uncertainty

The various tests described above give confidence in the accuracy of our analyses. Two USGS shale standards (SCo-1 and SGR-1b) were repeatedly analysed, including multiple dissolutions and chemical purification. Importantly, both were analysed using both double spikes described above, as a further test on sensitivity to inaccuracy of different aspects of our data reduction. The results are shown in Figure 7.

The internal reproducibility of an analysis is strongly dependent on the sample/background ratio (Fig. 2). Since the beam from a hydride generator is inherently unstable, due to the instability in reagent flow generated by the peristaltic pump, a low-intensity beam will be more strongly affected by background noise. This instability results in periodic beam fluctuations that will cause a degradation in the internal reproducibility which can be larger than the external reproducibility. Thus, for a <5% background contribution on ^{76}Se, the internal reproducibility is ±(0.03–0.1)‰ on $\delta^{82/76}$Se, whereas for a 10% background contribution the reproducibility is ±1‰ (Fig. 2). Samples were not run with a background contribution >5%. External uncertainty, based on repeated analyses (including dissolution and chemistry) of both USGS shales is ±0.17‰ (2sd) on $\delta^{82/76}$Se.

The $\delta^{82/76}$Se values of both SCo-1 ($\delta^{82/76}$Se = -0.22 ± 0.15, 2sd, n=18) and SGR-1 (0.25 ± 0.17, 2sd, n=16) from this study generally compare well to those published by Rouxel et al. (2002), Schilling et al. (2011) and Layton-Matthews et al. (2006, 2013). The results from SGR-1 from this study and those of Stüeken et al. (2013) are within analytical uncertainty of each other, but the population means of this study and that of Mitchell et al. (2012) are distinct from each other at the 95%

confidence level (student t-test, using data from Mitchell 2013, pers. comm.). These studies present a mix of double spike[7, 19] and sample-standard bracketing analyses[13, 17, 24, 25]. We note that the study of Rouxel et al. (2002) used a collision cell instrument that is no longer manufactured, which likely had a very different interference spectrum to correct. In addition, the different dissolution methods trialled in this study ("standard" HF-HNO_3 dissolution vs. high temperature ashing) resulted in identical isotope ratios within analytical uncertainty. The values for both shales using these different methods are reported in Table 2. Given that we have determined these values with two separate double spike inversion systems, we recommend these USGS shales as useful and easily accessible rock standards for assessing accuracy, or at least inter-study reproducibility, for future Se isotope analyses. We can, as yet, offer no explanation for the differences in published values of SGR-1, especially compared to those reported by Mitchell et al., 2012. Further work is needed to determine whether SGR-1 is isotopically heterogeneous, or whether some studies have unresolved analytical issues.

5.2 Desolvation analysis of Se isotopes

Generally the sensitivity of an MC-ICP-MS for Se is ~50 times better when using a hydride generator than a desolvation nebuliser such as a Cetac Aridus. However, we have discovered that doping a Se (or sulphur) solution with magnesium (in this case, the Mg isotope standard DSM-3) enhances the sensitivity when using "wet" (Elemental Scientific Inc. Apex) or "dry" (Cetac Aridus) plasma by up to a factor of 100-200 (Fig. 8a). The greatest Se sensitivity occurs at Mg/Se mass ratios of 10–20. When normalised to uptake rate (~50 μl/min), the sensitivity of Mg-doped Se using an Aridus is 1.6-1.9 times greater than that of a hydride generator. Here, Se was

introduced as selenate, in 2% HNO_3. Yield enhancement of Se when using ICP-MS has been reported when doping the solution with carbon[31] or in H_2SO_4- or HCl-based matrices[32]. However, these enhancements are only a factor of 2-3 (two orders of magnitude less than this study), and is thought to be due to the transfer of electrons to the C ions, because Se has a lower ionisation potential than C[31]. Clearly this effect cannot be causing the sensitivity enhancement by Mg, because Mg has a lower ionisation potential than Se. Recently, sulphate sensitivity has been enhanced by a factor of ~20, by doping with Na[33]. That study was also not able to explain these effects, and proposed that it might be related to the desolvating membrane. Our experiments with a membrane-less Apex, as well as a desolvating Aridus, now demonstrate this not to be the case. To our knowledge, sensitivity enhancement by Mg doping has not been reported to date. The enhancement effect also means that Se concentration analyses in any matrix containing Mg may be highly inaccurate unless either isotope dilution is used, or concentration analyses are performed by hydride generation ICP-MS.

The sensitivity enhancement effect of Mg could however be used to analyse Se isotope ratios in low concentration samples. Advantages of using desolvation introduction systems over hydride generation include faster washout times, more stable beams, and an introduction system that is more widely used. An obvious drawback is that in dry plasma mode, argide dimer production is higher. However, this can be overcome by tuning gas flows, torch positions and RF generator power until the background on ^{76}Se is sufficiently low (<5%) for corrections to be accurate.

Double-spike was used to analyse the Mg-doped Se solutions. Differences in mass bias style (i.e. deviations from exponential mass bias) due to Mg addition to pure Se solutions are not resolvable in double spike inversions. As shown in Figure

8b, mixtures of the NIST standard with amounts of spike yield consistent results whether run by hydride generator or with Mg-addition and desolvation, which implies that, whilst the relative importance of different interferences using the two techniques might change, our procedure corrects for these accurately.

The intensity of the main interferences (Ge and As) are little affected by Mg doping, and desolvation nebulisation is not an efficient means of generating Ge beams. Thus a solution with Ge/Se = 0.2, when doped with Mg, has a measured Ge/Se = 0.05. In contrast, the sensitivity of As when using desolvation nebulisation is not as poor as for Ge, and the yield of Mg-doped SeH is different from that of AsH in the same solution, so that the SeH yield cannot be used to correct for AsH. This means that a double spike scheme that avoids ^{76}Se is advisable, for example the alternative inversion scheme detailed in this study, or in other studies[19]. Nevertheless, this method provides the potential for Se isotope analysis by laboratories with no hydride generation facilities.

5.3 Mass Independent Fractionation of Selenium

Sulphur mass independent fractionation (MIF) has been reported in samples from the Archean, and is generally thought to reflect photolysis of S-bearing tropospheric gases by ultraviolet radiation and the production of elemental sulphur particles in the atmosphere[34-36]. Thus, the widespread occurrence of significant non-zero $\Delta^{33}S$ ($\Delta^{33}S = (^{33}S/^{32}S)_{sample}/(^{33}S/^{32}S)_{V\text{-}CDT}\text{-}[(^{34}S/^{32}S)_{sample}/(^{34}S/^{32}S)_{V\text{-}CDT}]^{0.515}$) in rocks deposited prior to ~2.4 Ga[34] suggests that atmospheric O_2 was $<10^{-5}$ of present atmospheric levels[37, 38], and that reducing gases such as methane or hydrogen were considerably more abundant than today[39]. Given the chemical similarities between S and Se, partly through the volcanic cycle[6], and the ability of both to form compounds

that are gases, it is possible that Se isotopes could demonstrate MIF in a manner similar to S isotopes.

To test the hypothesis that Se MIF may be preserved in Archean shales, we have performed Se isotope analyses on five Neoarchean shales from a well-preserved drill core (GKF01) from the ~2.65-2.5 Ga Ghaap Group, South Africa[40], all of which record large $\Delta^{33}S$ fractionations (-1.7 to +6.9‰; Table 3[41]). Our analyses were identical to those described above for hydride generation mass dependent fractionation, except that samples were not double-spiked, and new plasma interface cones were employed in the mass spectrometer that had not been used for any double spiked analyses. While no memory effect from spike tracer has been observed on the cones in this study, changing cones countered any such possibility. In addition, the hydride generator was thoroughly cleaned prior to analyses, and all sample introduction tubing was replaced. Finally, sample analyses were bracketed by analyses of NIST-3149, in order to be able to correct for any non-exponential law instrumental mass fractionation. Due to the potential mass-dependent fractionation effects of the chemistry, MDF results are not reported from these samples.

There are no MIF Se data reported in any previous studies. Those studies that have used SSB to determine mass-dependent fractionation (MDF)[4, 13, 17, 24, 25] neither report sufficient statistical detail nor, with one exception[13], the results of repeat analyses, making it impossible to retrospectively calculate the uncertainty of the MIF. In principal, SSB-determined MDF ratios may be used for reporting MIF, but care needs to be taken to propagate the uncertainties, and their correlations, to correctly determine the uncertainty in the MIF. In general, the correlations between the isotope ratios are such that explicit MIF measurements using internal normalisation are significantly more precise than MDF measurements. The study by Rouxel et al.

(2002), wherein isotope measurements on repeat analyses of a MERCK Se standard are reported, allows us one point of comparison of the uncertainty to our own MIF data. We have calculated the MIF on each analysis of the MERCK standard (excluding two that did not measure ^{77}Se, see table 4 in [13]) using the exponential fractionation law to normalise to ^{82}Se/^{78}Se yielding a reproducibility of ±0.20‰ (2σ, n=13) for MIF $\delta^{82/77}$Se compared to our MIF reproducibility of ±0.03–0.04‰ as detailed below.

Given the low relative intensities of interferences on ^{77}Se, ^{78}Se and ^{82}Se, the ^{82}Se/^{78}Se ratio was used to internally normalise the reported ^{82}Se/^{77}Se ratio, using the exponential mass bias law[42]. We have also examined the ^{82}Se/^{78}Se normalised ^{76}Se/^{77}Se ratio. We present our internally normalised results in epsilon form (deviation in parts per 10,000, to bring units in-line with other isotopic MIF results (e.g., [43]):

$$\varepsilon^{x/77}Se_{\frac{82}{78}} = \left(\frac{\left({}^{x}Se / {}^{77}Se_{\frac{82}{78}} \right)_{spl}}{\left({}^{x}Se / {}^{77}Se_{\frac{82}{78}} \right)_{std}} - 1 \right) \times 10^{4} \qquad (1)$$

where the normalising ratio is included as a subscript (i.e., ^{82}Se/^{78}Se)[43], and x refers to ^{76}Se or ^{82}Se, *spl* is the sample, and *std* the standard. The interferences on ^{76}Se (from Ge, As and ArAr) result in variable $\varepsilon^{76/77}Se_{\frac{82}{78}}$ Thus for 500 ng/g NIST-3149, $\varepsilon^{76/77}Se_{\frac{82}{78}}$ varies by ±1.2□, and for SGR-1b (n=2, chemistry =2) it varies by ±1.7□. This suggests that these interferences are also a large factor in the uncertainty on the double spike inversions described above. However the $\varepsilon^{82/77}Se_{\frac{82}{78}}$ ratio reproduces much better; the analytical uncertainty for NIST-3149 is ±0.31□, and for SGR-1b is ±

0.40□ (Table 3). This uncertainty is therefore likely to be the external reproducibility of our analyses, assuming that the Eocene SGR-1b does not exhibit any Se MIF.

The Archean shales exhibit a mean $\varepsilon^{82/77}Se_{\frac{82}{78}}$ of -0.39 ± 0.27□ (n=5). All shales (including SGR-1b) exhibit slightly negative $\varepsilon^{82/77}Se_{\frac{82}{78}}$ values relative to NIST-3149, which may suggest that either NIST-3149 itself is not typical of common terrestrial Se. This has been observed for several other highly purified standards analysed to high precision for MIF[43-45]. This effect is potentially as a function of the purification by non-exponential processes, and/or that during purification, a species other than the element is being fractionated (e.g. in this case selenate- or selenite-oxide rather than pure Se). In any case, the critical observation is that the Archean shales are within the range of SGR-1b, and therefore do not exhibit any resolvable mass independent fractionation, or correlation between $\varepsilon^{82/77}Se_{\frac{82}{78}}$ and $\Delta^{33}S$ (Fig. 9). This may be because Se gas-phase reactions are not photocatalysed in a mass independent manner under anoxic atmospheric conditions, but could also be due to homogenisation of an atmospheric Se MIF signal prior to preservation in the sediment[46]. In addition, oxidised Se gases tend to be less volatile than similar sulphur-based compounds.

6.0 Conclusions

This study presents data using two different double spikes and variably-spiked samples to accurately constrain selenium isotope ratios in two different USGS shale standards. Our measurements suggest that the $\delta^{82/76}Se$ ($^{82}Se/^{76}Se$ deviation from NIST-3149) values of SCo-1 = -0.22 ± 0.15‰ (n=18), and of SGR-1b = +0.25 ±

0.17‰ (n=16). Measurements obtained by other studies using a mix of double spike or sample-standard bracketing, generally agree well with our robustly defined values.

We also present a new method for measuring Se isotopes (for isotope dilution or isotope ratios) using desolvation or "moist" plasma. Doping Se solutions with Mg leads to an increase in Se sensitivity by a factor of 100-200, almost 2 times greater than the uptake-rate normalised sensitivity of a hydride generator.

Finally, we have assessed Archean shales that demonstrate sulphur mass independent isotope fractionation (MIF) for Se MIF. The $^{82}Se/^{77}Se$ ratios, normalised to $^{82}Se/^{78}Se$, show no significant deviations from analyses of the Eocene standard SGR-1b (-0.39 ± 0.27□, parts per 10,000), and no correlation with existing $\Delta^{33}S$ measurements in Archean samples. Thus, Se does not show resolvable MIF behaviour in samples that are likely candidates to record a strong variability in MIF signature.

Acknowledgments

The authors would like to thank Thomas Johnson and Kristin Mitchell for discussions on Se isotopes. Analyses were supported by NERC grant NE/F016832/1. PPvS is supported by NERC fellowship NE/I020571/1.

1. S. K. Clark and T. M. Johnson, *Journal of Environmental Quality*, 2010, **39**, 2200-2210. DOI: 10.2134/jeq2009.0380.
2. T. M. Johnson, *Chemical Geology*, 2004, **204**, 201-214. DOI: 10.1016/j.chemgeo.2003.11.015.
3. T. M. Johnson, M. J. Herbel, T. D. Bullen and P. T. Zawislanski, *Geochimica et Cosmochimica Acta*, 1999, **63**, 2775-2783. DOI: 10.1016/s0016-7037(99)00279-3.
4. O. Rouxel, Y. Fouquet and J. N. Ludden, *Geochimica et Cosmochimica Acta*, 2004, **68**, 2295-2311. DOI: 10.1016/j.gca.2003.11.029.
5. H. J. Wen and J. Carignan, *Geochimica et Cosmochimica Acta*, 2011, **75**, 1411-1427. DOI: 10.1016/j.gca.2010.12.021.
6. T. M. Johnson and T. D. Bullen, in *Geochimistry of Non-Traditional Stable Isotopes*, ed. C. M. Johnson, B. L. Beard and F. Albarede, Geochemical Society. 2004, pp. 289-317.

7. K. Mitchell, P. R. D. Mason, P. Van Cappellen, T. M. Johnson, B. C. Gill, J. D. Owens, J. Diaz, E. D. Ingall, G. J. Reichart and T. W. Lyons, *Geochimica et Cosmochimica Acta*, 2012, **89**, 302-317. DOI: 10.1016/j.gca.2012.03.038.
8. A. Fernandez-Martinez and L. Charlet, *Reviews in Environmental Science and Biotechnology*, 2009, **8**, 81-110.
9. A. S. Ellis, T. M. Johnson, M. J. Herbel and T. D. Bullen, *Chemical Geology*, 2003, **195**, 119-129. DOI: 10.1016/s0009-2541(02)00391-1.
10. M. J. Herbel, J. S. Blum, R. S. Oremland and S. E. Borglin, *Geomicrobiology Journal*, 2003, **20**, 587-602. DOI: 10.1080/713851163.
11. M. J. Herbel, T. M. Johnson, R. S. Oremland and T. D. Bullen, *Geochimica et Cosmochimica Acta*, 2000, **64**, 3701-3709. DOI: 10.1016/s0016-7037(00)00456-7.
12. T. M. Johnson and T. D. Bullen, *Geochimica et Cosmochimica Acta*, 2003, **67**, 413-419.
13. O. Rouxel, J. Ludden, J. Carignan, L. Marin and Y. Fouquet, *Geochimica et Cosmochimica Acta*, 2002, **66**, 3191-3199.
14. N. Elwaer and H. Hintelmann, *Analytical and Bioanalytical Chemistry*, 2007, **389**, 1889-1899. DOI: 10.1007/s00216-007-1537-z.
15. D. Savard, L. P. Bedard and S.-J. Barnes, *Talanta*, 2006, **70**, 466-571.
16. N. Elwaer and H. Hintelmann, *Journal of Analytical Atomic Spectrometry*, 2008, **23**, 733-743. DOI: 10.1039/b801673a.
17. E. E. Stüeken, J. Foriel, B. K. Nelson, R. Buick and D. C. Catling, *Journal of Analytical Atomic Spectrometry*, 2013, **28**, 1734–1749. DOI: 10.1039/c3ja50186h.
18. N. Elwaer and H. Hintelmann, *Journal of Analytical Atomic Spectrometry*, 2008, **23**, 1392-1396. DOI: 10.1039/b808645c.
19. K. Schilling, T. M. Johnson and W. Wilcke, *Soil Science Society of America Journal*, 2011, **75**, 1354-1364. DOI: 10.2136/sssaj2010.0377.
20. J. M. Zhu, T. M. Johnson, S. K. Clark and X. K. Zhu, *Chinese Journal of Analytical Chemistry*, 2008, **36**, 1385-1390.
21. J. M. Zhu, T. M. Johnson, S. K. Clark, X. K. Zhu and X. L. Wang, *Geochimica et Cosmochimica Acta*, 2014, **126**, 228–249.
22. H. Fan, H. Wen, R. Hu and H. Zhao, *Geochimica et Cosmochimica Acta*, 2011, **75**, 7725-7740. DOI: 10.1016/j.gca.2011.09.027.
23. T. R. Kulp and L. M. Pratt, *Geochimica et Cosmochimica Acta*, 2004, **68**, 3687-3701. DOI: 10.1016/j.gca.2004.03.008.
24. D. Layton-Matthews, M. I. Leybourne, J. M. Peter and S. D. Scott, *Journal of Analytical Atomic Spectrometry*, 2006, **21**, 41-49. DOI: 10.1039/b501704a.
25. D. Layton-Matthews, M. I. Leybourne, J. M. Peter, S. D. Scott, B. Cousens and B. M. Eglington, *Geochimica et Cosmochimica Acta*, 2013, **117**, 313–331.
26. J. F. Rudge, B. C. Reynolds and B. Bourdon, *Chemical Geology*, 2009, **265**, 420-431. DOI: 10.1016/j.chemgeo.2009.05.010.
27. J. Wang, T. X. Ren, H. Lu, T. Zhou and M. T. Zhao, *International Journal of Mass Spectrometry*, 2011, **308**, 65-70. DOI: 10.1016/j.ijms.2011.07.023.
28. J. Carignan and H. J. Wen, *Chemical Geology*, 2007, **242**, 347-350. DOI: 10.1016/j.chemgeo.2007.03.020.
29. Y. K. Chau and J. P. Riley, *Analytica Chimica Acta*, 1964, **33**, 36-49.
30. N. Elwaer and H. Hintelmann, *Talanta*, 2008, **75**, 205-214. DOI: 10.1016/j.talanta.2007.10.046.
31. E. H. Larsen and S. Sturup, *Journal of Analytical Atomic Spectrometry*, 1994, **9**, 1099-1105. DOI: 10.1039/ja9940901099.

32. K.-S. Park, S.-T. Kim, Y.-M. Kim, Y. Kim and W. Lee, *Bulletin of the Korean Chemical Society*, 2002, **23**, 1389-1393.
33. G. Paris, A. L. Sessions, A. V. Subhas and J. F. Adkins, *Chemical Geology*, 2013, **45**, 50–61.
34. J. Farquhar, H. M. Bao and M. Thiemens, *Science*, 2000, **289**, 756-758. DOI: 10.1126/science.289.5480.756.
35. J. Farquhar, J. Savarino, S. Airieau and M. H. Thiemens, *Journal of Geophysical Research-Planets*, 2001, **106**, 32829-32839. DOI: 10.1029/2000je001437.
36. J. Farquhar, N. P. Wu, D. E. Canfield and H. Oduro, *Economic Geology*, 2010, **105**, 509-533.
37. A. A. Pavlov and J. F. Kasting, *Astrobiology*, 2002, **2**, 27-41. DOI: 10.1089/153110702753621321.
38. M. H. Thiemens, in *Annual Review of Earth and Planetary Sciences*. 2006, vol. 34, pp. 217-262.
39. K. Zahnle, M. Claire and D. Catling, *Geobiology*, 2006, **4**, 271-283. DOI: 10.1111/j.1472-4669.2006.00085.x.
40. S. Schroder, J. P. Lacassie and N. J. Beukes, *South African Journal of Geology*, 2006, **109**, 23–54.
41. A. L. Zerkle, M. Claire, S. D. Domagal-Goldman, J. Farquhar and S. W. Poulton, *Nature Geoscience*, 2012, **5**, 359-363. DOI: 10.1038/ngeo1425.
42. W. Russell, D. A. Papanastassiou and T. Tombrello, *Geochimica et Cosmochimica Acta*, 1978, **42**, 1075–1090.
43. R. C. J. Steele, T. Elliott, C. D. Coath and M. Regelous, *Geochimica et Cosmochimica Acta*, 2011, **75**, 7906-7925. DOI: 10.1016/j.gca.2011.08.030.
44. R. W. Carlson, M. Boyet and M. Horan, *Science*, 2007, **316**, 1175–1178.
45. F. Moynier, A. Agranier, D. C. Hezel and A. Bouvier, *Earth and Planetary Science Letters*, 2010, **300**, 359–366.
46. J. Farquhar and B. A. Wing, *Earth and Planetary Science Letters*, 2003, **213**, 1-13. DOI: 10.1016/s0012-821x(03)00296-6.

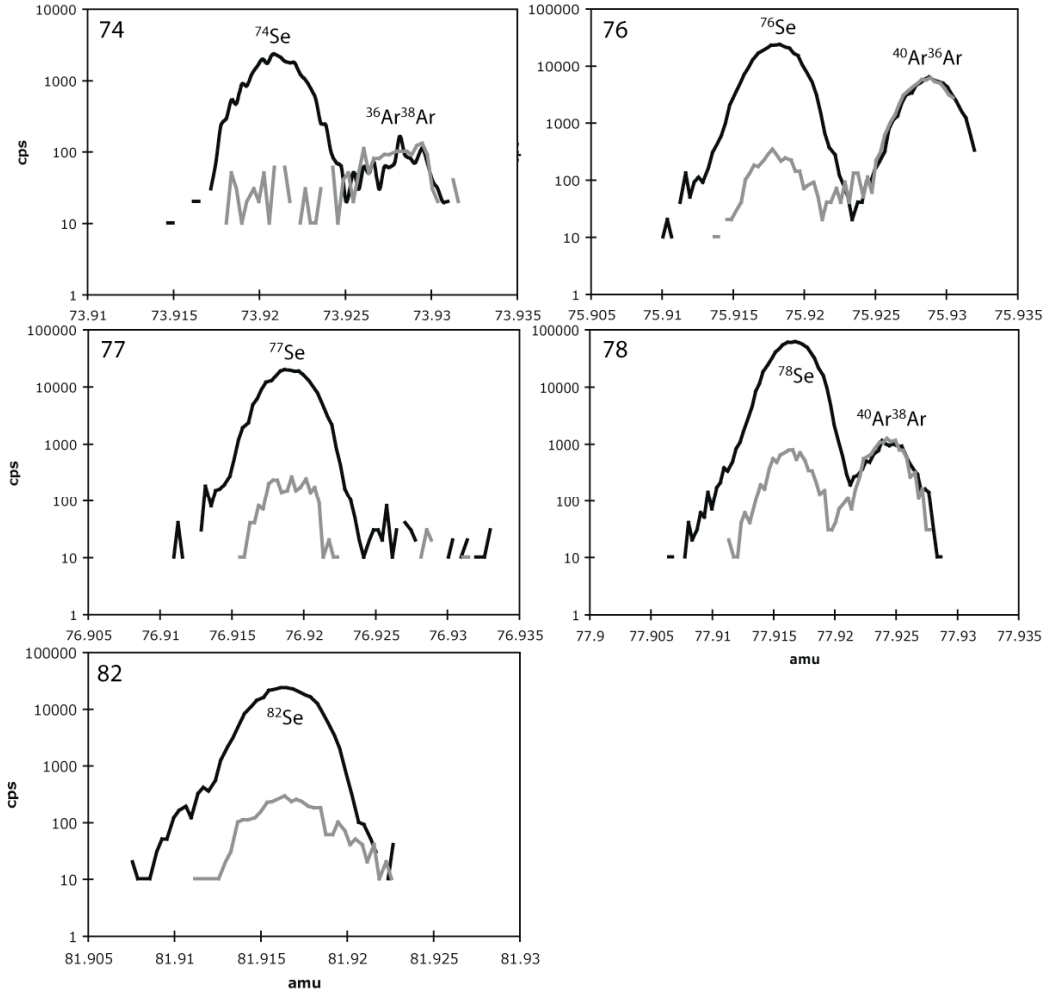

Figure 1

Se peaks determined at high resolution (M/ΔM ~ 10,000, 5-95% peak edge width) on an Element 2 HG-ICP-MS. Black lines represent the beam from a 25 ng/g NIST-3149 solution. Grey lines represent beams obtained when aspirating clean acid. The resolved argide peaks have identical intensities in the sample and in the clean acid solution, indicating that Se aspiration and hydride formation does not affect argide formation, and therefore that background subtraction is a viable form of argide correction.

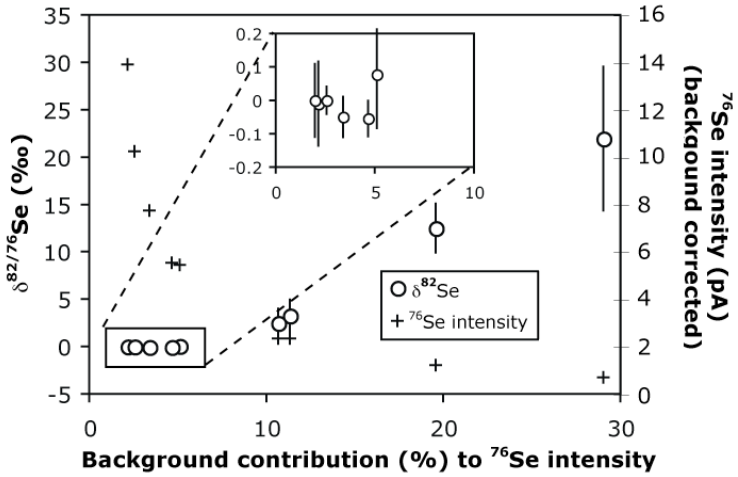

Figure 2
Se isotope ratios determined with decreasing Se intensity, and therefore increasing background contribution of $^{40}Ar^{36}Ar$. This demonstrates the minimum signal to noise ratio for accurate data when using ^{76}Se for the double spike inversion. The error bars represent the 2 s.e. of the analyses.

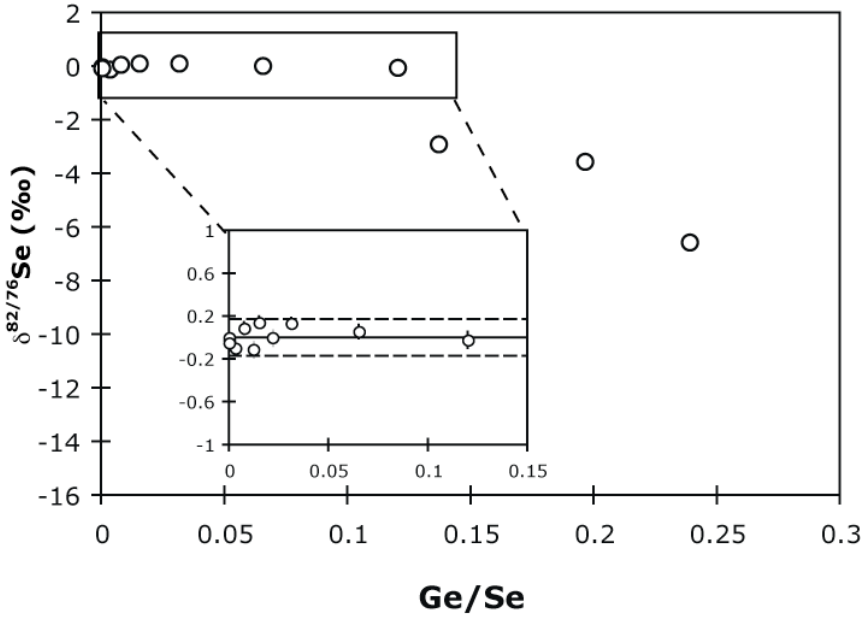

Figure 3
Ge doping experiments on NIST-3149. In the insert the solid line represents 0‰, and the dashed lines the external uncertainty (2 s.d.).

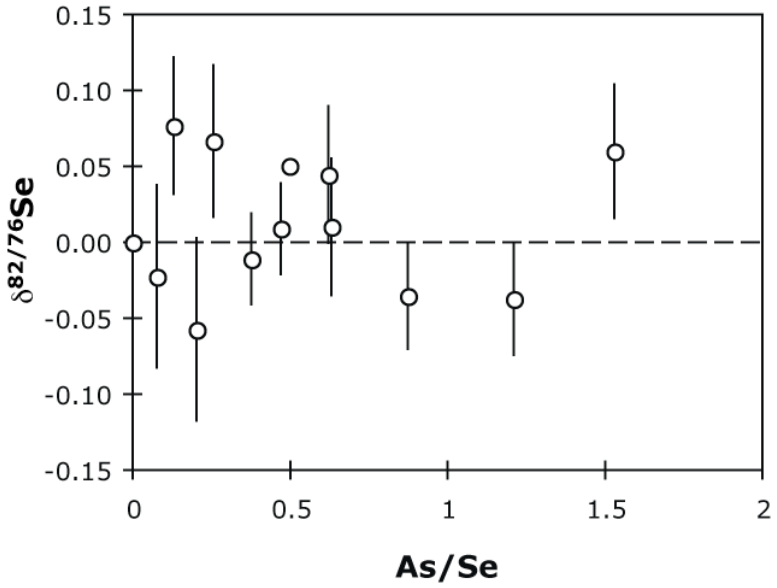

Figure 4
Arsenic doping experiments on NIST-3149. The data represent experiments at several different mass spectrometer tuning settings, and therefore different levels of hydride formation. The error bars represent the 2 s.e. internal uncertainty of the analyses.

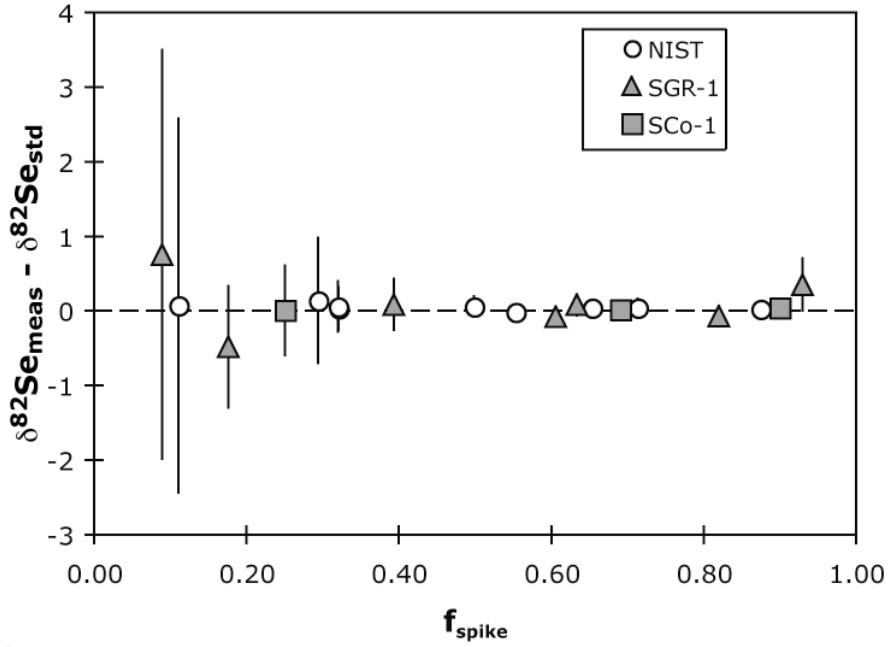

Figure 5

Results of variably spiking standards and samples. The approach is detailed in the text. Both SGR-1 and SCo-1 data have been differenced to their "true" $\delta^{82/76}$Se value, as detailed in Table 2, in order to directly compare these data to NIST and model data. This approach shows that both NIST and shale samples behave identically to each other, demonstrating that all interferences are corrected. The NIST data also indicate the ideal sample-spike mix, where the uncertainty is smallest (f_{spike} ~0.55–0.75).

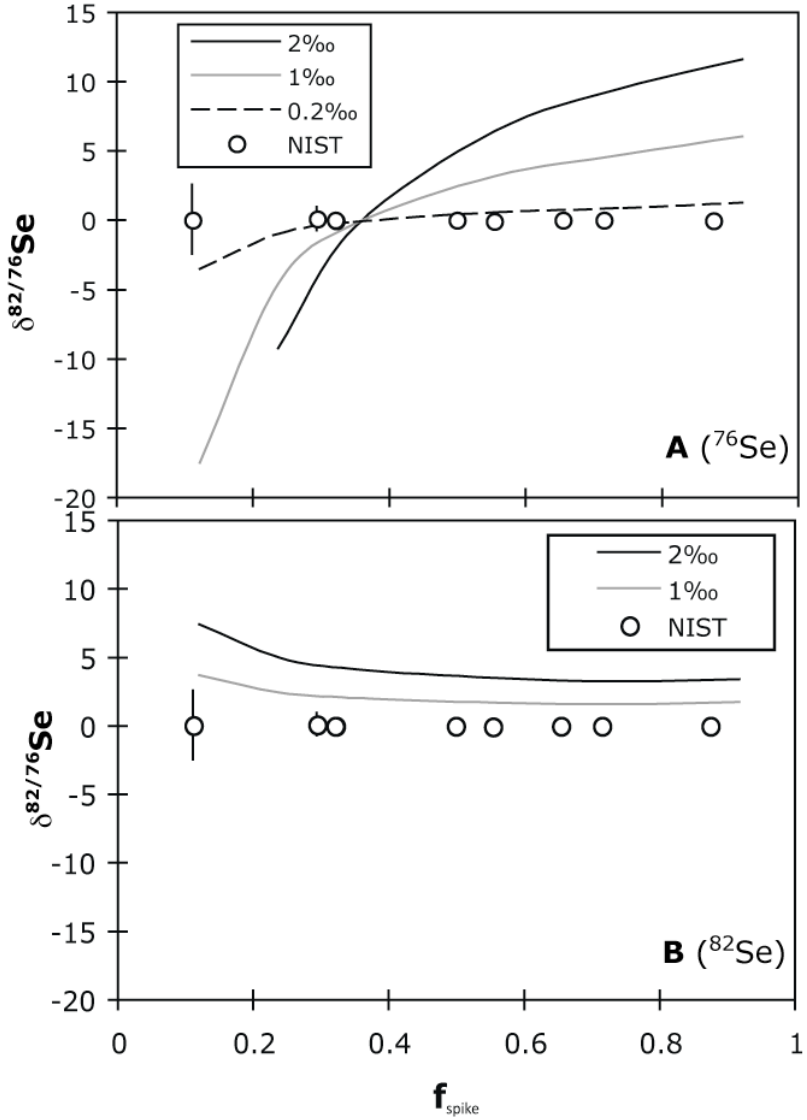

Figure 6
Modelled results for variable spiking (see Fig. 5) if interferences are left uncorrected. For example, the black lines show results for a 2‰ uncorrected interference on ^{76}Se (A) and ^{82}Se (B), respectively. The data from variably spiked NIST (Fig. 5) are shown for comparison.

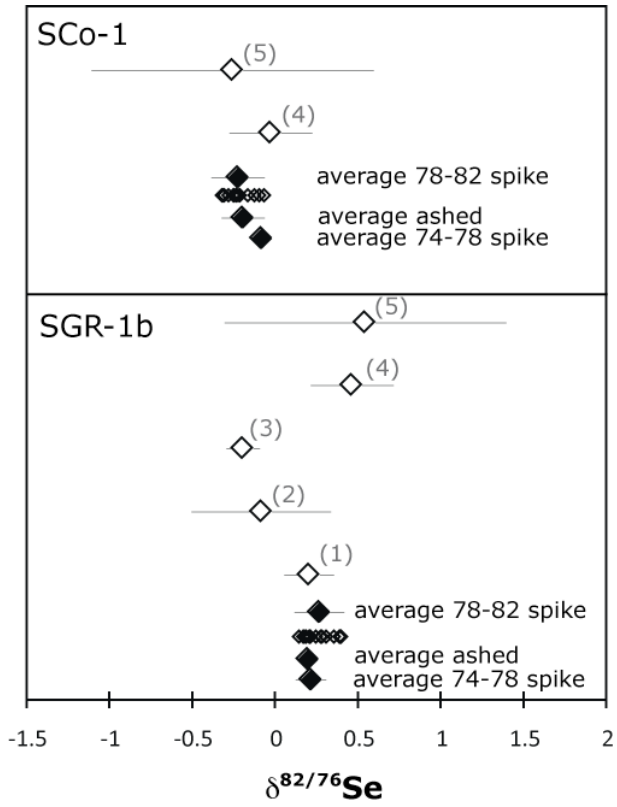

Figure 7

Results from this study's analyses of both USGS shales (closed symbols), compared to published values (open symbols). (1): Schilling et al., 2011; (2): Stüeken et al., 2013; (3): Mitchell et al., 2012; (4) Rouxel et al., 2002; (5) Layton-Matthews et al., 2006, 2013. The error bars in all cases represent the 2 s.d. analytical reproducibility. The small open diamonds represent this study's individual analyses.

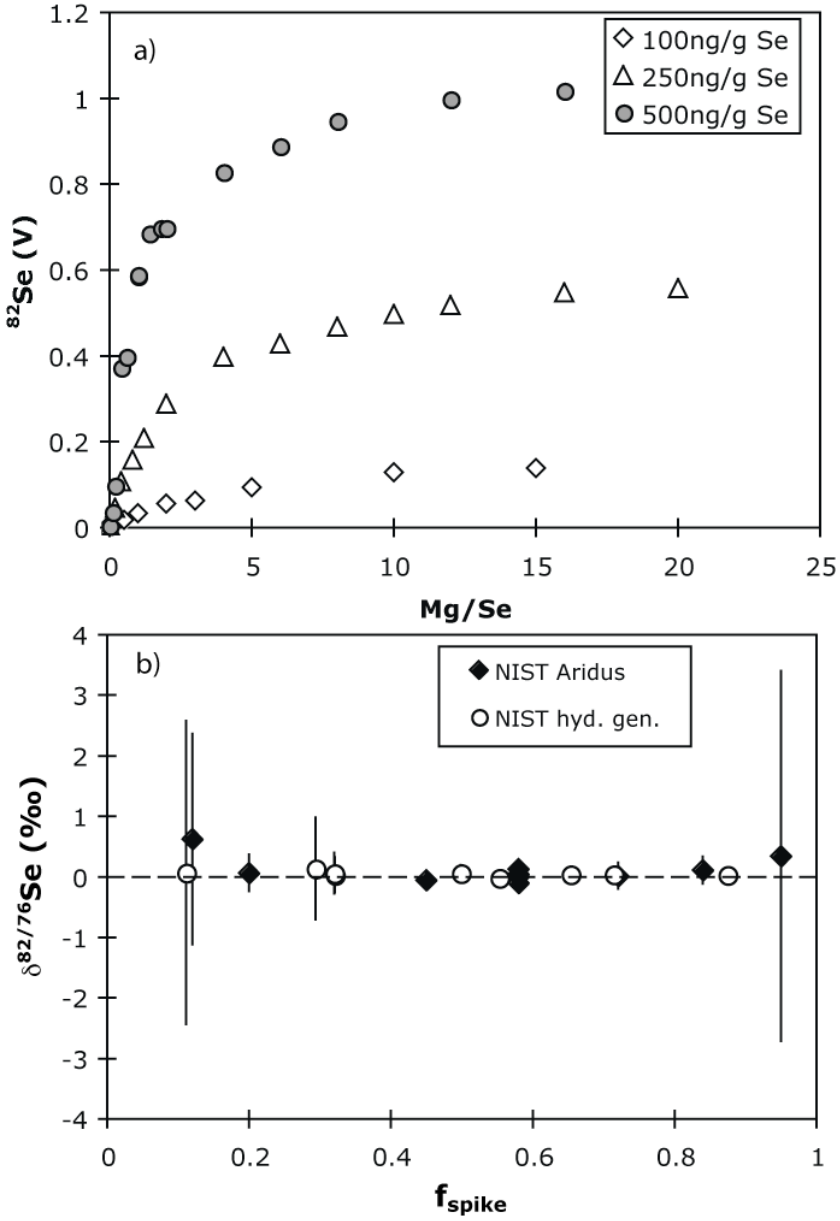

Figure 8. a) Mg doping of Se solutions when using an Aridus introduction system. Mg/Se is given as a mass ratio. b) Results of variably spiking Mg-doped NIST-3149, also using an Aridus. The error bars represent the 2s.e. internal reproducibility.

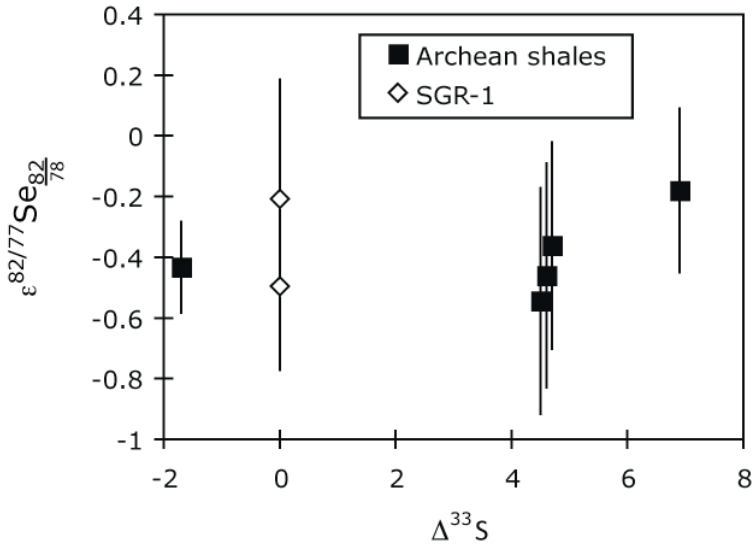

Figure 9. Mass independent Se isotopes (in parts per 10,000) plotted against mass independent S isotopes. The error bars on the individual data points represent 2 s.e internal reproducibility. The 2 s.d. external reproducibility can be observed from the repeated measurements of SGR-1b.

Cups	L4	L3	L2	L1	C	H1	H2	H3	H4
	^{73}Ge	^{74}Se	^{75}As	^{76}Se	^{77}Se	^{78}Se	^{80}Se	^{82}Se	^{82}SeH
natural		0.89%		9.36%	7.63%	23.78%	49.61%	8.73%	
Double spike 1		46%				54%			
Double spike 2						16%		84%	
Major interferences									
Explicitly corrected		^{74}Ge		^{76}Ge					
				^{75}AsH					
					^{76}SeH	^{77}SeH			
Background corrected		^{36}Ar^{38}Ar		^{40}Ar^{36}Ar		^{40}Ar^{38}Ar	^{40}Ar^{40}Ar		
				^{38}Ar^{38}Ar					
						^{78}Kr	^{80}Kr	^{82}Kr	^{83}Kr
					^{40}Ar^{37}Cl				
							^{79}BrH	^{81}BrH	

Table 1. Details of the cup configuration and double spikes used, as well as the main interferences on each mass.

	dissolution	n	$\delta^{82/76}$Se	2 sd	[Se] µg/g
SCo-1	standard	14	-0.23	0.16	
	ashing	3	-0.20	0.13	
^{74}Se-^{78}Se spike	standard	1	-0.09*		
	mean	18	-0.22	0.15	0.79
SGR-1b	standard	12	0.26	0.15	
	ashing	2	0.19	0.06	
^{74}Se-^{78}Se spike	standard	2	0.21*	0.09	
	mean	16	0.25	0.17	3.10

Table 2. Results of the two USGS shale standards analysed in this study. * indicates ratios converted to $\delta^{82/76}$Se from $\delta^{82/77}$Se. Unless indicated, results were obtained using a ^{78}Se-^{82}Se spike.

Sample	Formation	Δ^{33}S (‰)	$\varepsilon^{76/77}Se_{\frac{82}{78}}$ (‰)	2 se	$\varepsilon^{82/77}Se_{\frac{82}{78}}$ (‰)	2 se
SGR-1b			-1.654	0.416	-0.496	0.276
SGR-1b			-2.853	0.522	-0.208	0.393
GKF01						
Depth (m)						
832.1	U. Nauga Fm.	4.5	-1.489	0.720	-0.543	0.373
982	L. Nauga Fm.	4.6	-1.651	0.894	-0.460	0.370
1141.8	L. Nauga Fm.	6.9	-2.206	0.395	-0.180	0.270
1413.6	Monteville Fm.	-1.7	-1.871	0.250	-0.433	0.149
1462.3	Lokammona Fm.	4.7	-2.028	0.485	-0.361	0.340
				2 sd		2 sd
Mean Archean shales			-1.849	0.574	-0.395	0.274

Table 3. Se mass independent fractionation isotope ratios. $\Delta^{33}S$ data from Zerkle et al. (2012).

Appendix

Interference corrections for 78-82 double spiked samples

After on-peak blank subtraction the ion beam intensities ^{76}Tot, ^{77}Tot, ^{78}Tot and ^{82}Tot at masses 76, 77, 78 and 82 respectively are taken to be the sums of the contributions from: i) Se and Ge atomic ions and ii) SeH and AsH molecular ions, i.e.,

$$^{76}\text{Se} = {}^{76}\text{Tot} - {}^{76}\text{Ge} - \text{AsH} \quad (1)$$

$$^{77}\text{Se} = {}^{77}\text{Tot} - {}^{76}\text{SeH} \quad (2)$$

$$^{78}\text{Se} = {}^{78}\text{Tot} - {}^{77}\text{SeH} \quad (3)$$

^{82}Se suffers no contributions from these species. With the assumption of a single instrumental mass bias parameter, β (see Rudge et al., 2009), which applies to all species, the ion beam intensities ^{76}Ge, SeH and AsH in the above equations may be written in terms of the measured intensities of ^{73}Ge, ^{82}SeH and As thus,

$$^{76}Se = {}^{76}Tot - {}^{73}Ge[{}^{76}Ge/{}^{73}Ge]e^{\beta pGe} - As \cdot he^{\beta(pAsH - p_{83}^{SeH})} \quad (4)$$

$$^{77}Se = {}^{76}Tot - {}^{76}Se \cdot he^{\beta(p_{77}^{SeH} - p_{83}^{SeH})} \quad (5)$$

$$^{78}Se = {}^{78}Tot - {}^{77}Se \cdot he^{\beta(p_{78}^{SeH} - p_{83}^{SeH})} \quad (6)$$

where

$$h = {}^{82}\text{SeH}/{}^{82}\text{Se} \quad (7)$$

$$p^{Ge} = \ln\{\text{mass}({}^{76}\text{Ge})/\text{mass}({}^{73}\text{Ge})\} \quad (8)$$

$$p^{AsH} = \ln\{\text{mass(AsH)}/\text{mass(As)}\} \quad (9)$$

$$p_{83}{}^{SeH} = \ln\{\text{mass}({}^{82}\text{SeH})/\text{mass}({}^{82}\text{Se})\} \quad (10)$$

$$p_{77}{}^{SeH} = \ln\{\text{mass}({}^{76}\text{SeH})/\text{mass}({}^{76}\text{Se})\} \quad (11)$$

$$p_{78}{}^{SeH} = \ln\{\text{mass}({}^{77}\text{SeH})/\text{mass}({}^{77}\text{Se})\} \quad (12)$$

$[{}^{76}\text{Ge}/{}^{73}\text{Ge}]$ is the true Ge isotopic abundance ratio, assumed known.

Let,

$$m_1(\beta) = {}^{77}\text{Se}/{}^{76}\text{Se} \quad (13)$$

$$m_2(\beta) = {}^{78}\text{Se}/{}^{76}\text{Se} \quad (14)$$

$$m_3(\beta) = {}^{82}\text{Se}/{}^{76}\text{Se} \quad (15)$$

Using equations 4–6 we may write down expressions for these three isotopes ratios in terms of measured intensities, known constants and the instrumental mass bias, β. For the measurement of a mixture of sample and double-spike tracer we may write down three mixing relations,

$$m_i(\beta)e^{-\beta P_i} = \lambda T_i + (1-\lambda)n_i e^{-\alpha P_i}, \qquad (i = 1,2,3) \qquad (16)$$

where $P_i = \ln\{\text{mass}(^{xx}Se)/\text{mass}(^{76}Se)\}$ and xx=77, 78 and 82 for i = 1, 2, and 3 respectively, T_i is the isotopic ratio of the double spike tracer, α is the fractionation (parameter) of the sample relative to the reference ratio, n_i, and λ is the mixing parameter. These are the well-known sample-tracer mixing equations (see the Double Spike Toolbox (Rudge et al., 2009) for these well-established definitions and equations) with the mixture ratio, m_i, now a function of β as a result of the interference correction. we can solve these three equations for the three unknowns α, β and λ by means of standard numerical methods. The reported $\delta^{82/76}$Se is then given by,

$$\delta^{82/76}Se = (e^{-\alpha P_3} - 1) \times 10^3 \qquad (17)$$